QPSK-modulation Wireless Transmitter Based on Time-domain Coding Metasurface

Jun Wang[1,2,3], Junfeng Li[1], Xianglin Kong[1], Xiaoyi Wang[4], and Lei Zhao[1]

[1]School of Information and Control Engineering
China University of Mining and Technology, Xuzhou 221116, China
jun-wang@cumt.edu.cn, jflimax@163.com, xlkong@cumt.edu.cn, leizhao@cumt.edu.cn

[2]Science and Technology on Antenna and Microwave Laboratory
Xidian University, Xi'an 710071, China

[3]State Key Laboratory of Millimeter Waves, School of Information Science and Engineering
Southeast University, Nanjing 211189, China

[4]College of Electronic and Information Engineering
Tongji University, Shanghai 201804, China
xiaoyiwang@tongji.edu.cn

Abstract – In this paper, a wireless communication system based on time-domain digital coding metasurface with Quadrature Phase Shift Keying (QPSK) modulation is proposed. The aperture-coupled resonant rings on the metal patches of the metasurface elements create an asymmetry along the *x*-axis, resulting in a phase difference. The Field Programmable Gate Array (FPGA) is used to change the conduction and cutoff states of pin diodes, which can control the phase responses of the metasurface elements, forming four coding states. Within a certain period, the FPGA dynamically modulates the high and low levels, thus controlling the reflection characteristics of the metasurface. When the information is converted into a binary bitstream and written into the FPGA, represented by high and low levels, the baseband signal is modulated onto the carrier by the metasurface. This system replaces the functionality of mixers in traditional wireless communication systems, further simplifying the architecture of wireless communication systems. The overall system is demonstrated by an experiment with a picture transmitted and received in real time, showing promise in future low-cost wireless communication transmission systems.

Index Terms – Metasurfaces, time-domain digital coding, wireless communication.

I. INTRODUCTION

Wireless communication technology is becoming increasingly important in today's era, and people have higher requirements for communication systems' stability, transmission rate, and latency [1]. However, the increasing number of protocols and standards has led to a surge in costs and complexity in the hardware implementation process. To meet these requirements, more advanced technologies and equipment have been applied to achieve efficient wireless communication, such as large aperture antenna arrays [2], ultra-massive Multiple-in Multiple-out (MIMO) [3], large intelligent surfaces (LIS) [4], and terahertz (THz) band [5]. However, massive MIMO requires a very large number of radio frequency (RF) chains, and the design and manufacturing of high-performance RF components working in the high-frequency band are relatively complex. The potential of LIS to significantly enhance system capacity has been widely recognized. However, the large-scale deployment of these technologies faces obstacles such as high hardware costs, substantial energy consumption, and heat dissipation issues due to the use of numerous RF chains and operating frequency bands. Moreover, traditional transceiver architectures like homodyne or heterodyne, which have been successful in mobile communication systems, encounter challenges such as high costs and limited flexibility in future wireless communication systems. Therefore, the development of new transceiver architectures that offer flexibility and efficiency for future communication systems is of utmost importance.

Reconfigurable metasurfaces have been envisioned as a promising technology to address the challenges faced in transceiver design. In the past decade, new electromagnetic phenomena have been achieved by manipulating electromagnetic waves based on reconfigurable metasurface, enabling functions such as surface

Submitted On: October 16, 2023
Accepted On: June 26, 2024
https://doi.org/10.13052/2024.ACES.J.390805

impedance, polarization conversion, frequency selective surface, and orbital angular momentum [6–12]. Moreover, the utilization of embedded tunable devices like PIN diodes and varactor diodes has been proposed in the concept of time-domain digital coding metasurface [13–14]. These devices offer the ability to dynamically reconfigure metasurface functions in real time, presenting new opportunities for tailored manipulation of electromagnetic waves. By modulating the material interface, a mapping relationship can be established between the digital bits of baseband information and the phase, amplitude, or spectral profile of the metasurface unit cell. This capability holds great potential for creating a novel signal transmission framework, where digital signals can be directly encoded onto the carrier wave incident on the metasurface. This approach simplifies the system architecture of traditional transmitters. However, direct modulation of antennas, although achieving similar functionality, is limited in real-time data transmission due to its high complexity and low efficiency [15–20].

In this paper, a wireless communication system that utilizes a time-domain digital coding metasurface is proposed. This system enables Quadrature Phase Shift Keying (QPSK) modulation of baseband signals by manipulating the phase response of the metasurface during reflection at the interface. By establishing a mapping relationship between QPSK symbols and reflection coefficients, the system achieves precise control over the modulation process. This control is conveniently achieved by changing the on/off state of the PIN diode, which alters the time-varying reflection coefficients of the metamaterial surface. Experimental results conducted at 5.5 GHz validate the system's accuracy and reliability in wireless information transmission.

II. METASURFACE UNIT CELL THEORY AND DESIGN

A. Theory analysis

A conceptual description of the time-domain digital coding metasurface for wireless communication is presented in Fig. 1. When the metasurface is driven by the monochromatic wave $E_i(t)$, which is normally incident from the left side toward the reflective metasurface at the frequency $f = f_c$, the reflective wave of the metasurface can be represented as:

$$E_r(t) = \Gamma(t) \cdot E_i(t) = \Gamma(t) \cdot e^{j2\pi f_c t}, \quad (1)$$

where $E_r(t)$ and $\Gamma(t)$ stand for the reflected waveform and the transient reflection coefficient of the metasurface, respectively. Assuming that the metasurface is varying in a scale much slower than the incident wave to safely decouple the dispersion and time-varying effects

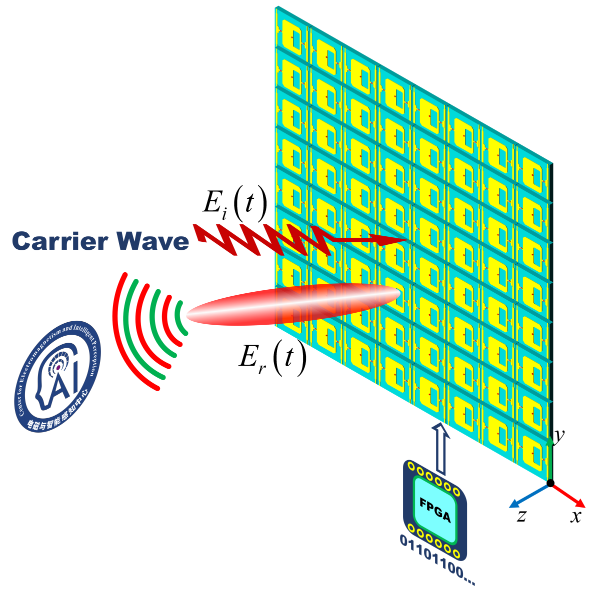

Fig. 1. Schematic diagram of wireless communication system based on reconfigurable digital coding metasurface.

of the reflective coefficient. The frequency domain of the reflective wave can be further obtained by performing Fourier transforming:

$$E_r(f) = \Gamma(f) * [\delta(f - f_c)] = \Gamma(f - f_c), \quad (2)$$

where $*$ denotes the convolution operation and $d(f)$ is the Dirac delta function. It can be seen that the reflection spectrum is highly dependent on the spectral profile of $\Gamma(f)$ from equation (2), indicating that the metasurface plays a similar role to the frequency mixer up-converting baseband signals to RF signals in the superheterodyne transceivers.

The proposed transmitter focuses on the scheme to realize the QPSK with the metasurface, using two PIN diodes to control the metasurface unit cell, achieving four encoding states. The binary data sequence of the reflection coefficient Γ_m can be represented based on different on/off states, as shown in equation (3):

$$\begin{aligned} \Gamma_0 &= \mathrm{OFF/OFF} \Leftrightarrow' 00', \\ \Gamma_1 &= \mathrm{ON/OFF} \Leftrightarrow' 01', \\ \Gamma_2 &= \mathrm{OFF/ON} \Leftrightarrow' 11', \\ \Gamma_3 &= \mathrm{ON/ON} \Leftrightarrow' 10'. \end{aligned} \quad (3)$$

By utilizing a time-domain 2-bit coding metasurface, it becomes feasible to encode each reflection coefficient Γ_m based on 2-bit binary digits.

B. Unit cell design

A 2-bit reconfigurable metasurface unit for the metasurface-based QPSK modulation is designed as

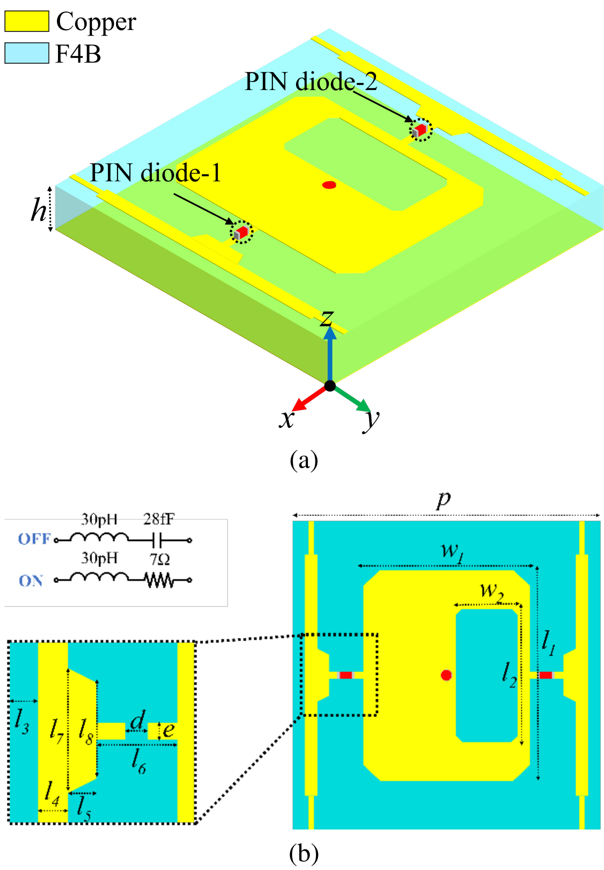

Fig. 2. (a) Structure of 2-bit metasurface unit cell and (b) top view of the metasurface unit cell with detailed parameters.

shown in Fig. 2. An aperture-coupled resonant ring is employed to create an asymmetry along the *x*-axis in the metal patches. Two PIN diodes are placed at the two sides of the patch. When the pin diodes patch switch to their ON states, a phase deviation occurs. By controlling the ON-OFF states of the pin diodes, a 90° phase is achieved in the metasurface unit response, creating four coding states for controlling the reflection characteristics of the reflective reconfigurable digital coding metasurface. These units will be used as "00", "01", "10", and "11" units for 2-bit encoding.

Figure 2 depicts the schematic diagram of the designed metasurface unit. As shown in Fig. 2 (a), the top layer of the unit consists of a square aperture resonant ring and a feeding line designed for the PIN diodes on both sides. The middle dielectric layer is made of F4B material with a dielectric constant of 2.55 and a loss tangent of 0.001. A metal via is placed in the center of the metal copper patch. By changing the voltage applied to the PIN diode loaded on the metasurface unit, different resonant states are generated when the *x*-polarized electromagnetic wave is incident on the metasurface, resulting in a change in the phase of the metasurface response. The pin diode chosen is MADP-000907-14020P by MACOM. This model of pin diode is also mentioned in [21]. The PIN diode of MADP-000907-14020P model produced by MACOM is selected for simulation and fabrication, which is conducive with a forward bias voltage, equivalent to a series lumped element with a resistance value of $R = 7\ \Omega$ and an inductance value of$L = 30$ pH, and is shut off with a reversed bias voltage, equivalent to a series lumped element with a capacitance value of $C = 28$ fF and an inductance value of$L = 30$ pH, as shown in Fig. 2 (b). The detailed structural parameters of the metasurface unit cell are listed in Table 1.

Table 1: Structure parameters of metasurface unit cell

Parameter	Length (mm)	Parameter	Length (mm)
h	2.54	14	1.2
p	27	15	1.5
wl	15	16	2.7
ll	16	17	6
*w*2	4	18	3
*l*2	9	d	0.3
*l*3	0.6	e	0.38

Figure 3 plots the reflection coefficients of the metasurface unit cell for *x*-polarized incident wave. As shown in Fig. 3 (a), by controlling the states of the two PIN diodes as OFF/OFF, ON/OFF, OFF/ON, and ON/ON, the resonant frequency of the unit cell increases from 5.4 GHz to 6.2 GHz while maintaining a reflection amplitude of more than 3 dB under *x*-polarized incident wave. This achieves a phase range coverage of 270° at the operating frequency of 5.5 GHz, as shown in Fig. 3 (b).

To further verify the effect of the PIN diode on the unit cell, Fig. 4 shows the surface current distribution of the unit cell in four different states of the PIN diodes at 5.5 GHz, which are labeled as states "00", "01", "10", and "11", respectively. It can be seen that when the PIN diodes are turned off, the current on the unit cell is very weak, while when the PIN diodes are turned on, the unit cell has a strong surface current, enabling the unit cell to change its resonant frequency and achieve the phase modulation. The proposed reconfigurable metasurface exhibits strong control over electromagnetic waves, making it a promising platform for dynamically manipulating the phase states.

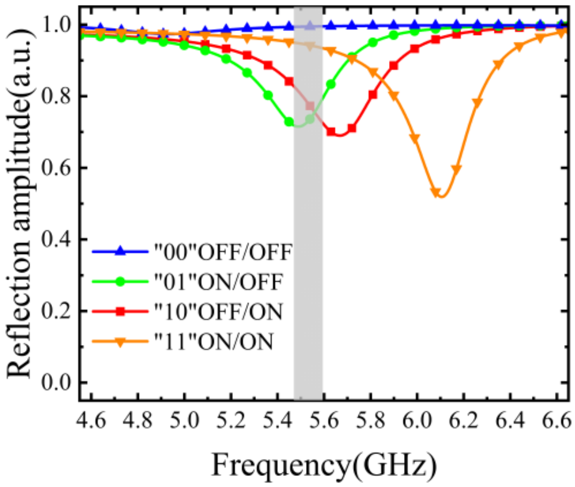

(a)

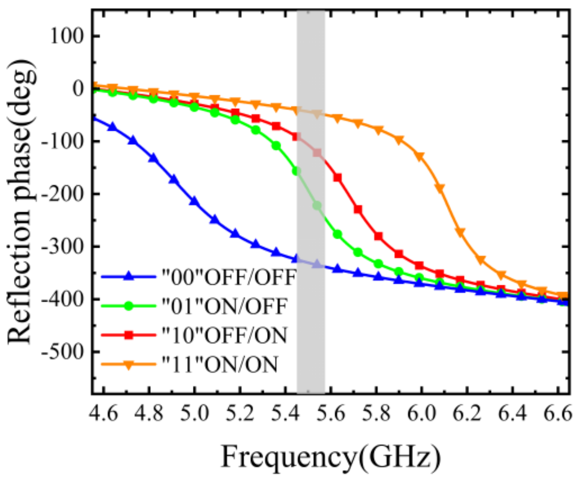

(b)

Fig. 3. Reflection coefficients of the metasurface unit cell for x-polarized incident wave: (a) amplitude response and (b) phase response.

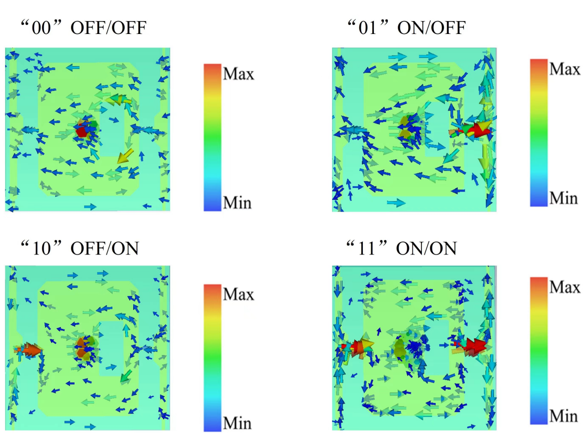

Fig. 4. Surface current distribution of the metasurface unit cell at different states.

III. EXPERIMENT OF WIRELESS COMMUNICATION SYSTEM

In order to verify the QPSK signal generated by the time-coding metasurface, a receiver using the Universal Software Radio Peripheral (USRP) is designed, which includes the following main modules, signal reception, automatic gain control, signal extraction, carrier synchronization, symbol synchronization, frame synchronization, phase offset correction, and demodulation, which are shown in Fig. 5.

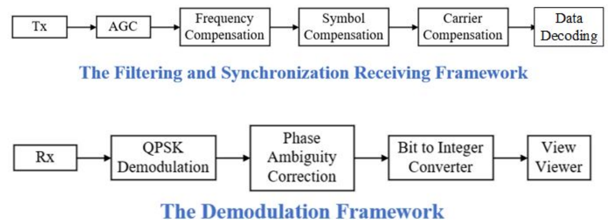

Fig. 5. QPSK receiving system model.

A metasurface-based communication system that can send and receive a picture is built. Figure 6 illustrates the entire wireless communication system, which

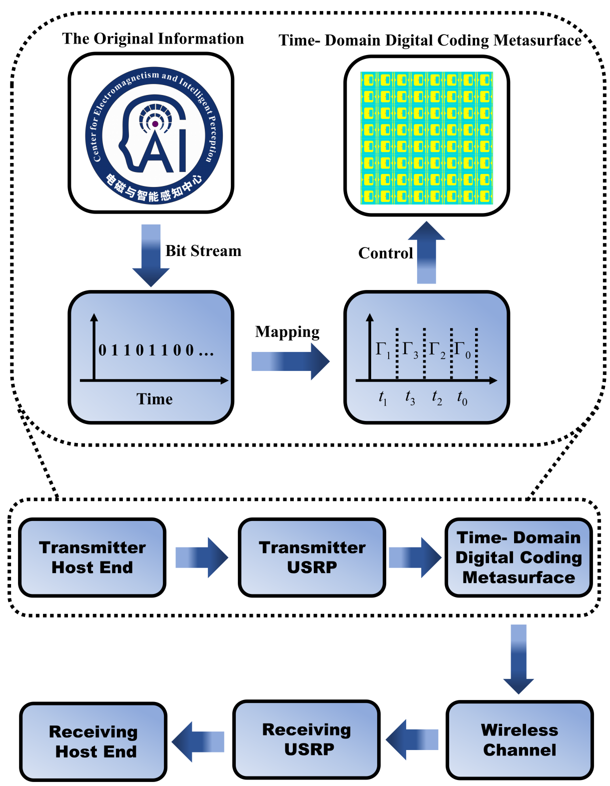

Fig. 6. Information transmission process diagram of the wireless communication system based on time-domain digital coding metasurface.

includes the transmitter consisting of the transmitter host, the transmitter-side USRP, and the time-domain digital coding metasurface and the receiver consisting of the receiver antenna, the receiver-side USRP, and the receiver host. In the transmitter, a single-tone signal is generated on the transmitter host. The picture information is firstly converted into bit stream and then mapped into QPSK modulation and finally used to control the time-domain digital coding metasurface. By adjusting the states of the PIN diodes through the modulating signal, the time-domain digital coding metasurface can modulate the carrier signal into a QPSK signal and scatter it into free space. At the receiver end, the signal is picked up by the receiving antenna and then processed by the receiving USRP and displayed on the receiver's host. In the proposed system, the time modulation period is chosen as 2.5 μs.

By extending the distance between the transmitter and receiver from 0.5 m to 1 m and increasing the data rate from 400 kbps to 800 kbps, the performance of the communication system can be evaluated under different conditions. The scatters plotted in Fig. 7 represent the constellation diagram of the received QPSK signals. As the data rate increases and the distance between the transmitter and receiver decreases, the performance of the communication improves gradually, and the scatter points of the constellation diagram converge. Additionally, the received and demodulated bitstream data at the receiver are shown in Fig. 8. To validate the proposed

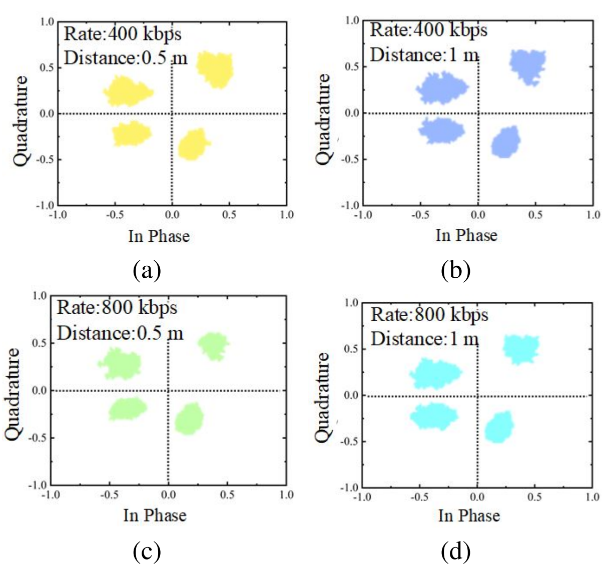

Fig. 7. Relationship between communication performance, transmission rate, and transmission distance. (a) Data rate: 400 kbps, distance: 0.5 m, (b) data rate: 400 kbps, distance: 1 m, (c) data rate: 800 kbps, distance: 0.5 m, and (d) data rate: 800 kbps, distance: 1 m.

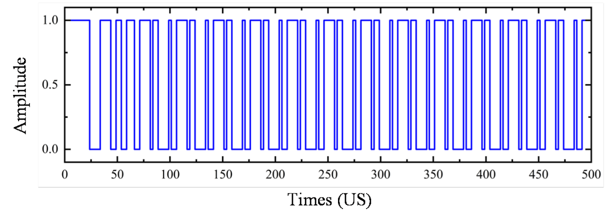

Fig. 8. Demodulated bitstream obtained.

information encoding scheme, the real-time image transmission experiments are conducted by using the time-domain digital coding metasurface wireless communication system in an indoor scenario, as shown in Fig. 9.

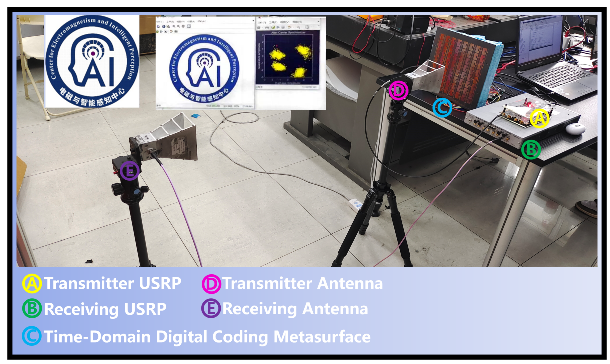

Fig. 9. Photograph of the wireless communication system based on time-domain digital coding metasurface.

The key parameters of the experiment based on time-domain digital coding metasurface are presented in Table 2. The transmitter is located on the left side of the workstation and consists of a DC power supply, Field Programmable Gate Array (FPGA), transmitter USRP, feeding antenna, and time-domain digital coding metasurface. The receiver is located on the right side of the workstation and consists of a receiving antenna, post-processing computer, and receiver USRP. The distance between the transmitter and receiver is 1 m. Experimental results show that the system performs well and may be further improved by enhancing the waveform of

Table 2: Selected key parameters of the designed wireless communication demo system based on a software-defined radio (USRP N310 & B210)

Parameter	Value
Working frequency	5.5 GHz
Modulation method	QPSK
Transmission rate	800 kbps
Frame size	960, 026 samples
Bit error rate	0.01

bias voltages and optimizing the metasurface unit cell to achieve better phase responses.

IV. CONCLUSION

In this paper, an experimental verification of a QPSK wireless communication system based on time-domain digital coding metasurface is presented. The proposed system demonstrates the feasibility and effectiveness of utilizing metasurfaces for wireless communication using QPSK modulation. Compared with traditional transmitters, the phase modulation of the baseband signal is directly completed by the metasurface, which simplifies the system architecture and eliminates the need for microwave devices such as mixers. The proposed metasurface-based wireless communication system is demonstrated by a real-time image transmission experiment in an indoor environment, which may find promising applications in future low-cost wireless communication systems.

ACKNOWLEDGMENT

This work was supported in part by the National Science Foundation of China under Grant 62201575, in part by the Science and Technology on Antenna and Microwave Laboratory Foundation under Grant 6142402220310, in part by the Open Project of State Key Laboratory of Millimeter Waves under Grant K202310.

REFERENCES

[1] T. Wild, V. Braun, and H. Viswanathan, “Joint design of communication and sensing for beyond 5G and 6G systems,” *IEEE Access*, vol. 9, pp. 30845-30857, Feb. 2021.

[2] E. De Carvalho, A. Ali, A. Amiri, M. Angjelichinoski, and R. W. Heath Jr., “Non-stationarities in extra-large-scale massive MIMO,” *IEEE Wireless Communications*, vol. 27, no. 4, pp. 74-80, Aug. 2020.

[3] V. Jamali, A. M. Tulino, G. Fischer, R. Muller, and R. Schober, “Intelligent surface-aided transmitter architectures for millimeter-wave ultra-massive MIMO systems,” *IEEE Open Journal of the Communications Society*, vol. 2, pp. 144-167, Dec. 2020.

[4] S. Hu, F. Rusek, and O. Edfors, “Beyond massive MIMO: The potential of data transmission with large intelligent surfaces,” *IEEE Transactions on Signal Processing*, vol. 66, no. 10, pp. 2746-2758, May 2018.

[5] M. Alibakhshikenari, E. M. Ali, M. Soruri, M. Dalarsson, M. Naser-Moghadasi, B. S. Virdee, C. Stefanovic, A. Pietrenko-Dabrowska, S. Koziel, S. Szczepanski, and E. Limiti, “A comprehensive survey on antennas on-chip based on metamaterial, metasurface, and substrate integrated waveguide principles for millimeter-waves and terahertz integrated circuits and systems,” *IEEE Access*, vol. 10, pp. 3668-3692, Jan. 2022.

[6] N. Yu, P. Genevet, M. A. Kats, F. Aieta, J.-P. Tetienne, F. Capasso, and Z. Gaburro, “Light propagation with phase discontinuities: Generalized laws of reflection and refraction,” *Science*, vol. 334, no. 6054, pp. 333-337, Oct. 2011.

[7] C. Pfeiffer and A. Grbic, “Metamaterial Huygens’ surfaces: Tailoring wave fronts with reflectionless sheets,” *Physical Review Letters*, vol. 110, no. 19, article 197401, May 2013.

[8] F. Falcone, T. Lopetegi, M. A. G. Laso, J. D. Baena, J. Bonache, M. Beruete, R. Marqués, F. Martín, and M. Sorolla, “Babinet principle applied to the design of metasurfaces and metamaterials,” *Physical Review Letters*, vol. 93, no. 19, article 197401, Nov. 2004.

[9] B. H. Fong, J. S. Colburn, J. J. Ottusch, J. L. Visher, and D. F. Sievenpiper, “Scalar and tensor holographic artificial impedance surfaces,” *IEEE Transactions on Antennas and Propagation*, vol. 58, no. 10, pp. 3212-3221, Oct. 2010.

[10] Y. Kawakami, T. Hori, M. Fujimoto, R. Yamaguchi, and K. Cho, “Low-profile design of metasurface considering FSS filtering characteristics,” *IEICE Transactions on Communications*, vol. 95, no. 2, pp. 477-483, Feb. 2012.

[11] E. Karimi, S. A. Schulz, I. De Leon, H. Qassim, J. Upham, and R. W. Boyd, “Generating optical orbital angular momentum at visible wavelengths using a plasmonic metasurface,” *Light: Science & Applications*, vol. 3, no. 5, article e167, May 2014.

[12] F. Li, H. Chen, Q. He, Y. Zhou, L. Zhang, X. Weng, H. Lu, J. Xie, and L. Deng, “Design and implementation of metamaterial polarization converter with the reflection and transmission polarization conversion simultaneously,” *Journal of Optics*, vol. 21, no. 4, article 045102, Mar. 2019.

[13] J. Y. Dai, J. Zhao, Q. Cheng, and T. J. Cui, “Independent control of harmonic amplitudes and phases via a time-domain digital coding metasurface,” *Light: Science & Applications*, vol. 7, no. 1, article 90, Nov. 2018.

[14] L. Zhang, X. Q. Chen, S. Liu, Q. Zhang, J. Zhao, J. Y. Dai, G. D. Bai, X. Wan, Q. Cheng, G. Castaldi, V. Galdi, and T. J. Cui, “Space-time-coding digital metasurfaces,” *Nature Communications*, vol. 9, no. 1, article 4334, Oct. 2018.

[15] S. Henthorn, K. L. Ford, and T. O’Farrell, “Bit-error-rate performance of quadrature modulation transmission using reconfigurable frequency

selective surfaces," *IEEE Antennas and Wireless Propagation Letters*, vol. 16, pp. 2038-2041, Apr. 2017.
[16] C. Liaskos, S. Nie, A. Tsioliaridou, A. Pitsillides, S. Ioannidis, and I. Akyildiz, "Realizing wireless communication through software-defined hypersurface environments," in *2018 IEEE 19th International Symposium on A World of Wireless, Mobile and Multimedia Networks (WoWMoM)*, pp. 14-15, Oct. 2018.
[17] C. Liaskos, S. Nie, A. Tsioliaridou, A. Pitsillides, S. Ioannidis, and I. Akyildiz, "A new wireless communication paradigm through software-controlled metasurfaces," *IEEE Communications Magazine*, vol. 56, no. 9, pp. 162-169, Sep. 2018.
[18] Y. Wang and A. Tennant, "Experimental time-modulated reflector array," *IEEE Transactions on Antennas and Propagation*, vol. 62, no. 12, pp. 6533-6536, Dec. 2014.
[19] X. Wang and C. Caloz, "Spread-spectrum selective camouflaging based on time-modulated metasurface," *IEEE Transactions on Antennas and Propagation*, vol. 69, no. 1, pp. 286-295, Jan. 2020.
[20] X. Wang and G. M. Yang, "Time-coding spread-spectrum reconfigurable intelligent surface for secure wireless communication: Theory and experiment," *Optics Express*, vol. 29, no. 20, pp. 32031-32041, Sep. 2021.
[21] Z. Qin, Y. F. Li, H. Wang, W. P. Wan, C. C. Li, Z. B. Zhu, Y. Cheng, S. Y. Li, H. Y. Chen, J. F. Wang, and S. B. Qu, "Polarization meta-converter for dynamic polarization states shifting with broadband characteristic," *Optics Express*, vol. 30, no. 11, pp. 20014-20025, May 2022.

Jun Wang was born in Jiangsu, China. He received the B.Eng. and M.S. degrees from Jiangsu Normal University, Xuzhou, China, in 2013 and 2017, respectively, and the Ph.D. degree in electromagnetic field and microwave technology from Southeast University, Nanjing, in 2021. From 2015 to 2016, he was with the Department of Electronic and Electrical Engineering, Nanyang Technological University of Singapore, as a Research Associate.

He joined the China University of Mining and Technology, Xuzhou, China, in 2021. He has authored or co-authored over 30 referred journal and conference papers. His current research interests include the design of RF/microwave antennas and components.

Junfeng Li was born in 1998 in Chongqing, China. He is currently pursuing a master's degree at the China University of Mining and Technology, Xuzhou, China.

His research direction is metasurface communication and software-defined radio.

Xianglin Kong (Member, IEEE) was born in Shandong, China, in 1995. He received the M.S. degree in information and communication engineering from China University of Mining and Technology (CUMT), Xuzhou, China, in 2021. He is currently pursuing the Ph.D. degree in information and communication engineering at CUMT, Xuzhou, China.

His research interests include microwave absorber, frequency selected surface, and vortex metasurface.

Xiaoyi Wang (Member, IEEE) received the B.S. degree in electronic science and technology from the University of Electronic Science and Technology of China (UESTC), Chengdu, China, in 2011, the M.S. degree in communication and information system from Fudan University, Shanghai, China, in 2014, and the Ph.D. degree in electrical engineering from Polytechnique Montréal, Montréal, QC, Canada, in 2020. He is currently a Research Professor with Tongji University, Shanghai. His research interests include all fields of theoretical, computational, and applied electromagnetics, with a strong emphasis on metamaterials and metasurfaces. Dr. Wang was a recipient of the Student Paper Competition Award of the IEEE International Symposium on Antennas and Propagation (AP-S) in 2019 and the International Union of Radio Science (URSI) Young Scientist Award in 2020.

Lei Zhao received the B.S. degree in mathematics from Jiangsu Normal University, China, in 1997, and the M.S. degree in computational mathematics and the Ph.D. degree in electromagnetic fields and microwave technology from Southeast University, Nanjing, China, in 2004 and 2007, respectively.

He joined the China University of Mining and Technology, Xuzhou, China, in 2019, where he is currently a Full Professor. From September 2009 to December 2018, he worked with Jiangsu Normal University, Xuzhou, China. From August 2007 to August 2009, he worked with the Department of Electronic Engineering, The Chinese University of Hong Kong, as a Research Associate. From February 2011 to April 2011, he worked with the Department of Electrical and Computer Engineering, National University of Singapore, as a Research Fellow. From September 2016 to September 2017, he worked with the Department of Electrical and Computer Engineering, University of Illinois at Urbana-Champaign, Champaign, IL, USA, as a Visiting Scholar. He has authored or coauthored more than 100 refereed journal and conference papers. His current research interests include spoof surface plasmon polaritons theory and its applications, RF/microwave antenna and filter design, computational electromagnetics, and electromagnetic radiation to human's body.

Dr. Zhao serves as an Associate Editor for *IEEE Access*, an Associate Editor-in-Chief for *Applied Computational Electromagnetics Society (ACES) Journal* and a reviewer for multiple journals and conferences including the *IEEE Trans. on Microwave Theory and Techniques, IEEE Trans. Antennas and Propagation, IEEE Antennas and Wireless Propagation Letters, Applied Computational Electromagnetics Society (ACES) Journal*, and other primary electromagnetics and microwave related journals.